

Design and Implementation of a Backstepping-Sliding mode Attitude Controller of a Satellite in processor in the Loop Test Bed using Reaction Wheels

Alireza Fazlyab¹, Farhad Fani Saberi², Mansour Kabganian³

¹Department of Mechanical Engineering, Amirkabir University of Technology

²Space Science and Technology Institute, Amirkabir University of Technology

³Department of Mechanical Engineering, Amirkabir University of Technology

-----ABSTRACT-----

In this paper, a robust attitude control algorithm is developed based on backstepping-sliding mode control for a satellite using four reaction-wheels. In this method, the actuator dynamics has been considered to design the controller and asymptotic stability of the proposed algorithm has been proven based on Lyapunov theory. Then, in order to evaluate the performance of the proposed algorithm, a low-cost real-time processor in the loop test bed is provided to real-time assessing the attitude control algorithm. In this test bed, real-time modeling of satellite dynamics, disturbances and reaction-wheels are achieved in a simulator computer and the control algorithm performance is investigated by implementing it in an electronic board of the test bed.

Keywords: Attitude, Backstepping-Sliding mode, Reaction wheel, Satellite, Processor in the loop.

Date of Submission: 10 June 2017



Date of Accepted: 30 June 2017

I. INTRODUCTION

A spacecraft requires several subsystems to achieve its mission successfully. Attitude determination and control system (ADCS) is one of the most crucial subsystems of a spacecraft. The major tasks of attitude control system are to provide the capability of high maneuverability, high pointing stability and attitude accuracy for the satellite. This subsystem has different parts including, sensors, actuators, control algorithm and electronic control board. The control algorithm is an important part of ADCS that provides commands for actuators.

Difficult problems in the design of control algorithm for such a complex dynamics system are due to the inherent nonlinearities of the model because of large angle maneuvers, uncertainties and unknown environmental disturbances. Among the research that has been done recently, there are a number of techniques that can deal with the control problems of such a complex dynamics system from classical PID control to adaptive control e.g. optimal control (Chelaru, et al., 2011), sliding mode control (Qinglei, 2008; Jin, et al., 2009; Qinglei, 2009), adaptive control (Moradi, 2013; Shahravi, et al., 2006; Guan, et al., 2005), robust control such as variable structure control (VSC) which are designed based on Euler angle errors or quaternion error vector.

The control algorithms in (Song, et al., 2014; Hu, 2009; Bošković, et al., 2001; Qinglei, et al., 2013) are based on variable structure control (VSC). Robustness is one of the most distinguishing properties of VSC systems. The VSC of multi axial spacecraft for large-angle rotational maneuvering has been studied in (Vadali, 1986; Dwyer, et al., 1987). In (Robinett & Parker, 1996; Wu, et al., 2011), a sliding mode control method has been presented for command tracking of spacecraft maneuvers based on Euler parameters. In (Vadali, 1986; Lu, et al., 2012), a sliding attitude control algorithm based on variable structure control has been designed using quaternion parameters. In (Ramirez & Dwyer, 1986), a sliding mode control technique has been developed for spacecraft pointing and regulation using Rodriguez (Gibbs vector) representation. Moreover in (Marandi & Modi, 1987; Shuster, 1993), sliding mode controller has been developed based upon the modified Rodriguez parameters which provides large angle maneuvers for a satellite. But in these methods, the effects of actuator dynamics like maximum torque limitation, delay in response, actuator and external disturbances have not been considered. Moreover, due to high cost and high risk of complex systems such as satellites, functional tests of most subsystems are highly desirable before launch. One solution to achieve functional tests of ADCS is to use processor in the loop (PIL) approach, where is a low cost and applicative test bed (Bolandi, et al., 2012).

In this paper, a backstepping-sliding mode attitude controller will be designed based on variable structure control (VSC) using four reaction wheels in a tetrahedron configuration. In this method the dynamics model of

actuators has been considered in order to design the controller and then asymptotic stability of the proposed algorithm has been proven in the presence of reaction wheels dynamics model based on lyapunov theory. To show the effect of considering the actuator dynamics in designing the controller, the simulation results of proposed backstepping-sliding will be compared with two different sliding mode controller. Then processor in the loop test bed will be designed and manufactured to evaluate the performance of the proposed attitude control algorithm in a real-time condition. The presented test bed is capable of real-time assessing the attitude backstepping-sliding mode control algorithm. In this test bed, real-time modeling of satellite dynamics, environmental disturbances and reaction wheels and gyros are achieved in a simulator computer and the proposed control algorithm performance is investigated by implementing it in an electronic control board of the processor in the loop test bed.

II. DYNAMICS AND KINEMATICS OF SATELLITE

The general equation to describe the attitude motion of a rigid satellite in space (Euler equations) in the presence of reaction wheels is described as follows (Sidi, 1997).

$$J \dot{\underline{\omega}} = -[\underline{\omega} \times] J \underline{\omega} + \underline{u} + T_{EXT} \tag{1}$$

Where, $\underline{\omega} = [\omega_x \ \omega_y \ \omega_z]^T$ is the angular velocity of spacecraft with respect to body reference frame, $\underline{u} \in R^3$ and $T_{EXT} \in R^3$ represent the control torques used for controlling the attitude and the external unknown differentiable disturbances, respectively. Here $J = I - C I_w C^T$, where I represents the inertia tensor of satellite and $I_w = \text{diag}\{I_{w1}, I_{w2}, I_{w3}, I_{w4}\}$ is the moment of inertia of the reaction wheels which are arranged in a pyramid configuration about the spacecraft yaw axis as shown in Figure 1. The orientation matrix of the above four-wheel pyramid configuration represented by a 3×4 matrix (C) which is considered as follow:

$$C = \begin{bmatrix} \cos \alpha \sin \beta & -\sin \alpha \sin \beta & -\cos \alpha \sin \beta & \sin \alpha \sin \beta \\ \sin \alpha \sin \beta & \cos \alpha \sin \beta & -\sin \alpha \sin \beta & -\cos \alpha \sin \beta \\ \cos \beta & \cos \beta & \cos \beta & \cos \beta \end{bmatrix} \tag{2}$$

Where α and β are considered as $\alpha = 45^\circ$ and $\beta = 54.74^\circ$.

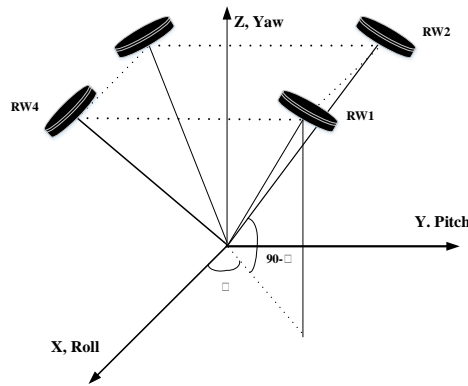


Figure 1. Four reaction wheels configuration

In order to represent the kinematics equation of the satellite we will use quaternion as follow (Crassidis & Markley, 1996):

$$\dot{\underline{q}}_v = \frac{1}{2} \left(q_4 I_{3 \times 3} + [\underline{q}_v \times] \right) \underline{\omega}, \quad \dot{q}_4 = -\frac{1}{2} \underline{q}_v^T \underline{\omega} \tag{3}$$

Here, the unit quaternion $(\underline{q}_v, q_4) \in R^3 \times R$ represents the attitude orientation of the spacecraft and satisfies the constraint $\underline{q}_v^T \underline{q}_v + q_4^2 = 1$, where $\underline{q}_v := [q_1, q_2, q_3]^T \in R^3$ is the vector part, $q_4 \in R$ is the scalar component. $[\underline{a} \times]$ is an operator on any vector $\underline{a} = [a_1 \ a_2 \ a_3]^T$ such that (Lu, et al., 2012):

$$[\underline{a} \times] = \begin{bmatrix} 0 & -a_3 & a_2 \\ a_3 & 0 & -a_1 \\ -a_2 & a_1 & 0 \end{bmatrix} \tag{4}$$

III. REACTION WHEEL MODEL

A reaction wheel fundamentally is a flywheel with a vehicle-fixed axis and a DC motor, designed to operate at zero bias. The dynamical behavior of reaction wheel originates from the response of the flywheel. When a control signal is input to a reaction wheel system, the largest limitation is caused by the dc-motor. According to this argument, the spacecraft dynamics is controlled by torque u applied by the reaction wheel actuator, and the actuator dynamics is controlled by the input voltage of the reaction wheel. To generate this torque by the reaction wheel, the voltage must be controlled. This is done by the design the attitude controller by involving the dynamics of the motor actuator. The differential equation for the armature of the DC motor circuits is given by (Hu, 2012).

$$L_a \dot{I}_a + R_a I_a + K_b \Omega = v \tag{5}$$

Where R_a , L_a , K_b , Ω , I_a and v are the armature resistance, the armature inductance, the back EMF constant, the angular velocity of motor, the armature current and applied armature voltage, respectively. On the other hand, the torque developed by the motor might be regarded as directly proportional to the armature current by motor torque constant (K_m) as follow:

$$u = K_m I_a \tag{6}$$

By substituting Eq. (6) in Eq. (5), we can define a general MIMO linear reaction wheel model by Eq. (7).

$$\frac{L_a}{K_m} \dot{u} + \frac{R_a}{K_m} u + K_b \Omega = v \Rightarrow T \dot{u} + Au + d = v \tag{7}$$

Where $u \in \mathbb{R}^M$ is a vector of actual control input, T is a diagonal square matrix with positive time constants, hence $T = T^T > 0$ and d is the limited internal disturbances and A is a positive constant. The disturbances caused by reaction wheel that are most effective in attitude control accuracy and stability of satellite includes: Dynamic Imbalance (U_d), Static Imbalance (U_s), Bearing Disturbances (t_{rb}), motor torque ripple (t_r) and disturbances caused by coulomb friction and viscous friction ($T_f + T_v$). These disturbances are applied directly to the satellite as an external disturbance (T_{EXT}) and effect on accuracy of attitude control and stability of satellite, so that the satellite dynamics in presence of reaction wheel model can be represent as follow:

$$\begin{cases} \dot{\omega} = J^{-1} ([J\omega \times] \omega) + J^{-1} u + J^{-1} T_{EXT} \\ T \dot{u} + Au + d = v \end{cases} \tag{8}$$

This dynamics will be considered to develop a robust controller in the next section and system stability will be evaluated in the presence of the proposed controller.

IV. BACKSTEPPING-SLIDING MODE CONTROLLER DESIGN

In this section a 3-axis attitude controller will be designed in two steps:

Step 1. Sliding mode attitude controller without considering reaction wheel dynamics model

Step 2. Backstepping-sliding mode attitude controller with considering actuator dynamics model

Then the results are compared to illustrate the effectiveness of the backstepping-sliding mode attitude controller in the presence of reaction wheel dynamics model and uncertainties.

4.1 Error Dynamic

Let $q_e = [q_{ve} \quad q_{4e}]^T$ denote relative attitude error from a desired reference frame to the body-fixed reference frame of the spacecraft. Then one may have:

$$q_e = q \otimes q_d^{-1} \tag{9}$$

Where q_d^{-1} is the inverse of the desired quaternion and \otimes is the quaternion multiplication operator. For any given two groups of quaternion, the relative attitude error is obtained by

$$\begin{bmatrix} \dot{q}_{ve} \\ \dot{q}_{4e} \end{bmatrix} = \frac{1}{2} \begin{bmatrix} q_{4e} I_{3 \times 3} + [q_{ve} \times] \\ -q_{ve}^T \end{bmatrix} \underline{\omega}_e(t) \quad \text{and} \quad \underline{\omega}_e = \underline{\omega} - \underline{\omega}_d \quad (10)$$

Where $\underline{\omega}_d$ represent desired angular velocity of the body which is assumed equal to zero, therefore

$$\underline{\omega}_d = \underline{0} \rightarrow \underline{\omega}_e = \underline{\omega} \quad (11)$$

Hence, the rate of angular velocity can be obtained as follow:

$$\dot{\underline{\omega}}_e = \dot{\underline{\omega}} = -J^{-1} [\underline{\omega} \times] J \underline{\omega} + J^{-1} \underline{u} + J^{-1} T_{EXT} \quad (12)$$

4.2 Sliding mode attitude controller without considering reaction wheel dynamics model

In this section a sliding mode attitude controller has been designed without considering actuator dynamics model. For this purpose, we will show sliding mode control law in form Eq. (13) can stabilize the origin of the plant (Eq. (1) and Eq. (3)).

$$\underline{u} = [\underline{\omega} \times] \hat{J} \underline{\omega} - \frac{1}{2} \hat{J} C \left(q_{4e} I_{3 \times 3} + [q_{ve} \times] \right) \underline{\omega} - \beta(\underline{\omega}, q_e) \text{sat} \left(\frac{s}{\varepsilon} \right) \quad (13)$$

Where $\beta(\underline{\omega}, q_e)$ is the upper bound for system uncertainties and $\text{sat} \left(\frac{s}{\varepsilon} \right)$ is shown in Eq. (14):

$$\text{sat} \left(s_i, \varepsilon_i \right) = \begin{cases} 1 & \text{for } s_i > \varepsilon_i \\ s/\varepsilon & \text{for } |s_i| < \varepsilon_i \\ -1 & \text{for } s_i < -\varepsilon_i \end{cases} \quad (14)$$

At first a linear sliding surface in vector form is defined in Eq. (15) as follow:

$$\underline{s} = \underline{\omega} + C \underline{q}_{ve} \quad (15)$$

Where $\underline{s} = [s_1, s_2, s_3]^T \in R^3$ and $C = \text{diag} [c_1, c_2, c_3]$ witch $c_i > 0, i = 1, 2, 3$ is scalar. The derivative of the sliding surface combined with Eq. (10) and Eq. (12) lead to the following:

$$\dot{\underline{s}} = \dot{\underline{\omega}} + C \dot{\underline{q}}_{ve} = -J^{-1} [\underline{\omega} \times] J \underline{\omega} + J^{-1} \underline{u} + J^{-1} T_{EXT} + \frac{1}{2} C \left(q_{4e} I_{3 \times 3} + [q_{ve} \times] \right) \underline{\omega} \quad (16)$$

In order to decrease chattering phenomenon and energy consumption we divided control input into continuous and switching components as follow:

$$\underline{u} = \underline{u}_{con} + \underline{u}_{swi} \quad (17)$$

So \underline{u}_{con} is obtained as follow:

$$\underline{u}_{con} = [\underline{\omega} \times] \hat{J} \underline{\omega} - \frac{1}{2} \hat{J} C \left(q_{4e} I_{3 \times 3} + [q_{ve} \times] \right) \underline{\omega} \quad (18)$$

In order to find switching (uncertainty) component \underline{u}_{swi} has been substituted in Eq. (16) as follow:

$$\dot{\underline{s}} = -J^{-1} [\underline{\omega} \times] J \underline{\omega} + J^{-1} [\underline{\omega} \times] \hat{J} \underline{\omega} + \frac{1}{2} C \left(q_{4e} I_{3 \times 3} + [q_{ve} \times] \right) \underline{\omega} - \frac{1}{2} J^{-1} \hat{J} C \left(q_{4e} I_{3 \times 3} + [q_{ve} \times] \right) \underline{\omega} + J^{-1} T_{EXT} + J^{-1} \underline{u}_{swi} \quad (19)$$

We assume the inertia matrix is in the form $J = \hat{J} + \Delta J$, where \hat{J} , selected nonsingular, is the known constant matrix and ΔJ denotes the uncertainties. So, the Eq. (19) is rewritten as:

$$\dot{\underline{s}} \stackrel{def}{=} \underline{\delta} + J^{-1} \underline{u}_{swi}, \quad \underline{\delta} = -J^{-1} [\underline{\omega} \times] \Delta J \underline{\omega} + \frac{1}{2} J^{-1} \Delta J C \left(q_{4e} I_{3 \times 3} + [q_{ve} \times] \right) \underline{\omega} + J^{-1} T_{EXT} \quad (20)$$

For determining \underline{u}_{swi} the upper bound of $J \underline{\delta}$ must be specified. Hence, $\alpha(\underline{\omega}, q_e)$ is assumed as the upper bound of $J \underline{\delta}$, and consequently the switching component has been obtained as follow:

$$\underline{u}_{swi} = -\beta(\underline{\omega}, q_e) \text{sign}(\underline{s}) \quad (21)$$

Where $\beta(\underline{\omega}, q_e) \geq \alpha(\underline{\omega}, q_e) + \beta_0$. In this step in order to avoid the chattering phenomenon the “sign” function has been replaced with “sat” function and the total control command is obtained as follow:

$$\underline{u} = [\underline{\omega} \times] \hat{J} \underline{\omega} - \frac{1}{2} \hat{J} C \left(q_{4e} I_{3 \times 3} + [q_{ve} \times] \right) \underline{\omega} - \beta(\underline{\omega}, q_e) \text{sat} \left(\frac{s}{\varepsilon} \right) \quad (22)$$

and

$$sat(s_i, \varepsilon_i) = \begin{cases} 1 & \text{for } s_i > \varepsilon_i \\ s/\varepsilon & \text{for } |s_i| < \varepsilon_i \\ -1 & \text{for } s_i < -\varepsilon_i \end{cases}$$

Now in order to prove the asymptotic stability of the system, we consider a Lyapunov candidate function as

$$V_1(s) = \frac{1}{2} \underline{s}^T \underline{s}, \text{ thus } \dot{V}_1(\underline{s}) \text{ is given by} \tag{23}$$

$$\begin{aligned} \dot{V}_1(\underline{s}) &= \underline{s}^T \dot{\underline{s}} = \underline{s}^T [\underline{\delta} + J^{-1} \underline{u}_{swi}] \leq \|\underline{s}\| \|\underline{\delta}\| + \underline{s}^T J^{-1} \underline{u}_{swi} \\ &\leq \|\underline{s}\| \|\underline{\delta}\| - \underline{s}^T J^{-1} \beta(\underline{\omega}, q_e) \text{sign}(\underline{s}) \leq \|\underline{s}\| \{ \|\underline{\delta}\| - J^{-1} \beta(\underline{\omega}, q_e) \} \\ &\leq \|\underline{s}\| \|J^{-1}\| \{ \|J\| \|\underline{\delta}\| - \beta(\underline{\omega}, q_e) \} \leq -\|\underline{s}\| \|J^{-1}\| \|\beta_0\| = -W(\underline{s}) \end{aligned}$$

$W(\underline{s})$ is a positive definite function, so $\dot{V}_1(t)$ is negative definite and asymptotic stability has been proved. The simulation results of designed controller in presence of reaction wheel dynamics model leads to an unexpected overshoots and converging time. Hence in the next section a new attitude controller in presence of reaction wheel dynamics model will be design.

4.2 Backstepping sliding mode attitude controller with considering actuator dynamics model

In this section the actuator dynamics model is considered in designing attitude controller. In order to design the controller in this situation, the designed sliding mode controller must be modify as follow: Consider Eq. (1) as dynamics equation of a spacecraft and Eq. (7) as the reaction wheel dynamics model. We will show a backstepping-sliding mode attitude control law in Eq. (24) can stabilize the origin.

$$\underline{v} = T [-k_1 \underline{z} + \underline{\phi}(\underline{\omega}, q_e) + T^{-1} A \underline{u} + T^{-1} d] \tag{24}$$

where T is a diagonal square matrix with positive time constants, $\underline{\phi}(\underline{\omega}, q_e)$ is an ideal stabilizing control feedback for Eq. (1), \underline{u} is actual control torque applied to the spacecraft, $\underline{z} = \underline{u} - \underline{\phi}$ and the relationship between \underline{u} and \underline{v} is given by Eq. (7). Now, spacecraft and reaction wheel dynamics are shown by Eq. (25) after applying a transformation in form of $\underline{v} = T(\underline{w} + T^{-1} A \underline{u} + T^{-1} d)$.

$$\begin{cases} \dot{\underline{\omega}} = J^{-1} (-[\underline{\omega} \times] J \underline{\omega} + T_{EXT}) + J^{-1} \underline{u} \\ \dot{\underline{u}} = \underline{w} \end{cases} \tag{25}$$

Now we are going to find a function $\underline{\phi}(\underline{\omega})$ in such a way that the spacecraft dynamics is stabilized. In this regard Eq. (25) can be rewrite in form of Eq. (26) which is similar to the spacecraft model.

$$\begin{cases} \dot{\underline{\omega}} = J^{-1} (-[\underline{\omega} \times] J \underline{\omega} + T_{EXT} + \underline{\phi}(\underline{\omega})) + J^{-1} (\underline{u} - \underline{\phi}(\underline{\omega})) \\ \dot{\underline{u}} = \underline{w} \end{cases} \tag{26}$$

It should be considered that the stability proof for the first term at right side Eq. (26) is achieved in section **Error! Reference source not found.**4.2 by using the following control law:

$$\underline{\phi}(\underline{\omega}, q_e) = [\underline{\omega} \times] \hat{J} \underline{\omega} - \frac{1}{2} \hat{J} C (q_{4e} I_{3 \times 3} + [q_{ve} \times]) \underline{\omega} - \beta(\underline{\omega}, q_e) sat\left(\frac{s}{\varepsilon}\right) \tag{27}$$

With changing variables in form of $\underline{z} = \underline{u} - \underline{\phi}$ and $\underline{p} = \underline{w} - \dot{\underline{\phi}}$, Eq. (26) will change into Eq. (28) in which the internal dynamics will be asymptotically stable.

$$\begin{cases} \dot{\underline{\omega}} = J^{-1} (-[\underline{\omega} \times] J \underline{\omega} + T_{EXT} + \underline{\phi}(\underline{\omega})) + J^{-1} \underline{z} \\ \dot{\underline{z}} = \underline{w} - \dot{\underline{\phi}}(\underline{\omega}) = \underline{p} \end{cases} \tag{28}$$

In order to prove the asymptotic stability of the system, we choose an augmented positive definite Lyapunov function as Eq. (29) and \dot{V}_a can be achieved as Eq. (30):

$$V_a = \frac{1}{2} \underline{s}^T \underline{s} + \frac{1}{2} \underline{z}^T \underline{z} \tag{29}$$

$$\dot{V}_a = \underline{s}^T \dot{\underline{s}} + \underline{z}^T \dot{\underline{z}} = \underline{s}^T (\underline{\delta} + J^{-1} \underline{u}_{swi}) + \underline{z}^T \underline{p} \leq -W(\underline{s}) + \underline{z}^T \underline{p} \tag{30}$$

By choosing \underline{p} in form of Eq. (31), \dot{V}_a will be a negative definite function. Therefore asymptotic stability of the whole system has been satisfied.

$$\underline{p} = -k_1 \underline{z} \Rightarrow \dot{V}_a \leq -W(\underline{s}) - k_1 \underline{z}^T \underline{z} < 0 \tag{31}$$

Here k_1 is a positive constant. So the control input (\underline{v}) in Eq. (24) will provide system stability in presence of actuator dynamics model. **Error! Reference source not found.** shows the proposed backstepping-sliding mode controller compared with the designed sliding mode controller (section 4.2) and sliding mode controller presented in (Crassidis & Markley, 1996) to demonstrate the effect of actuator dynamics model in designing the controller. Here desired Euler angles are assumed $\psi_d = 0^\circ, \theta_d = 25^\circ, \phi_d = 20^\circ$.

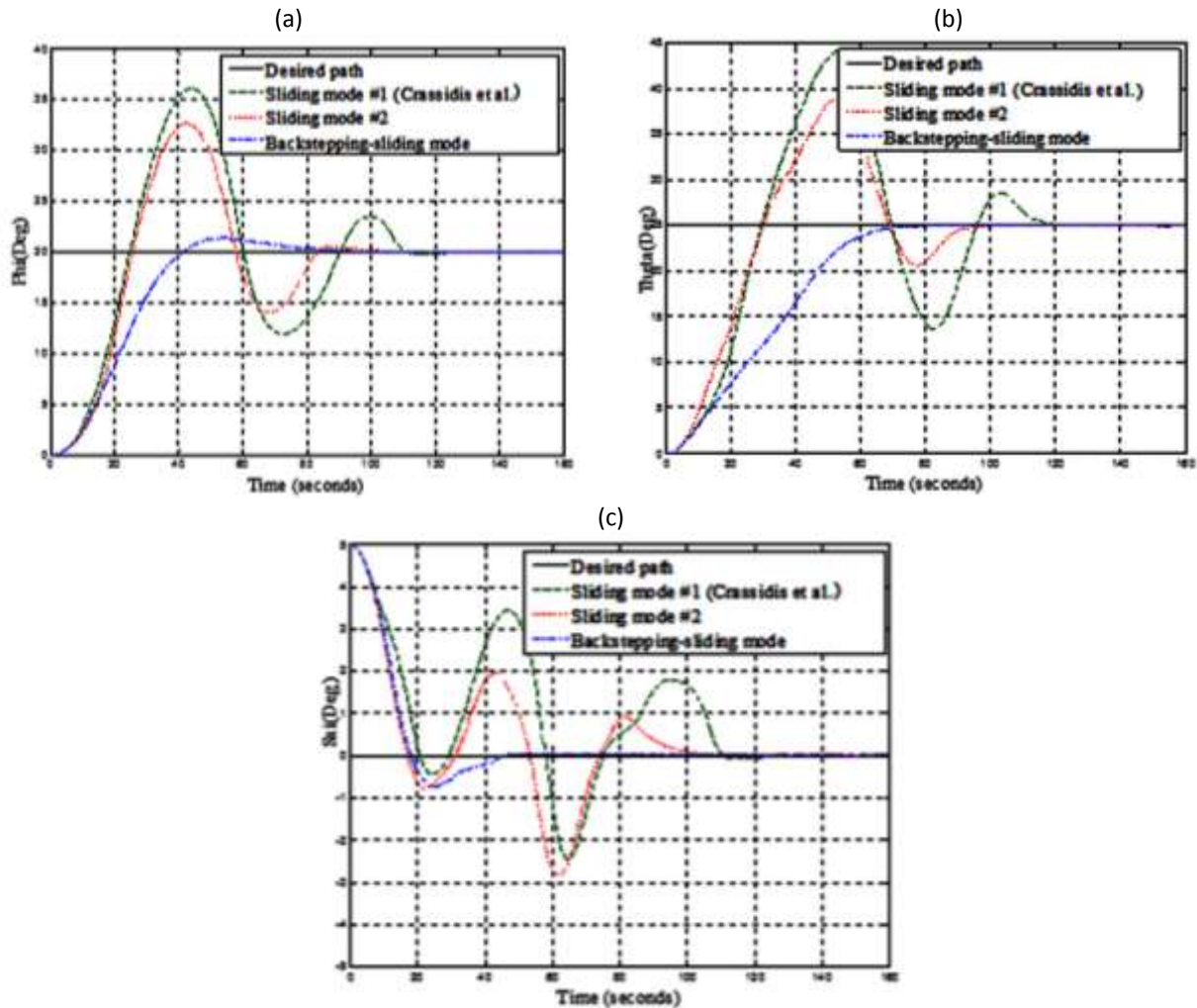


Figure 2. comparison of proposed controller with two sliding mode controller in the presence of actuator dynamics a) roll axis b) pitch axis c) yaw axis.

The results show, the controllers which designed without considering actuator dynamics, because of limitation in maximum torque of reaction wheel, delay time in response and inertial disturbances in reaction wheels have more overshoots and later converge to the desired path. But the backstepping-sliding mode controller because of considering reaction wheel dynamics in designing the controller, have no overshoot and reach the desired path more quickly. In the next section, the processor in the loop test bed for implementing of the backstepping-sliding mode controller will be presented.

V. PROCESSOR IN THE LOOP TEST BED

In this section, a processor in the loop test bed will be proposed to evaluate the performance of the designed attitude control algorithm in a real-time condition. Configuration of the processor in the loop contains three main

parts including: simulator computer, on-board electronics and an interface circuit for exchanging data between simulator computer and on-board electronics. The tasks of simulator computer can be expressed as: 1) modeling of orbital motion of satellite, rotational motion of satellite, environmental disturbances and actuators and sensors dynamics 2) providing a graphical convenient user interface for monitoring system performance.

Accurate modeling of satellite dynamics and space conditions has major role in design of test bed. For satisfying this requirement, a processor simulator is implemented in SIMULINK environment of MATLAB. In this simulator, accurate simulation of orbital motion of satellite, rotational motion of satellite, disturbances torque applied to the satellite, accurate model of reaction wheels and gyro are implemented. In this simulator, modeling is done based on high fidelity mathematical models, e.g. modeling of orbital dynamics is done based on KEPLER equation for Elliptical orbits (Sidi, 1997). Modeling of satellite attitude is implemented based on Euler's equations in (Sidi, 1997). Modeling of reaction wheels are implemented based on equation in (Bolandi, et al., 2011). Also to modeling disturbances, four common disturbances in low Earth orbit are considered including, gravity gradient, aerodynamic, geomagnetic and solar radiation torques (Wertz, 1978).

After implementing simulator model, next step is to execute simulator model in real-time mode. For this purpose capabilities of MATLAB and LABVIEW are used simultaneously. Simulation interface toolkit of LABVIEW includes a tool for MATLAB Real Time Workshop that converts simulation model into the C code. Then by using VISUAL C++, C code generated is converted into Dynamic Link Library (DLL) model. This model is capable to recall in LABVIEW and implementation of real-time simulation model. Graphical user interface is designed in LABVIEW and it is possible in this user interface to select satellite specifications, initial attitude and orbital parameters. Also it provides capability to monitor attitude of satellite, output of reaction wheels in real time condition. Figure 1 shows designed graphical user interface in LABVIEW.

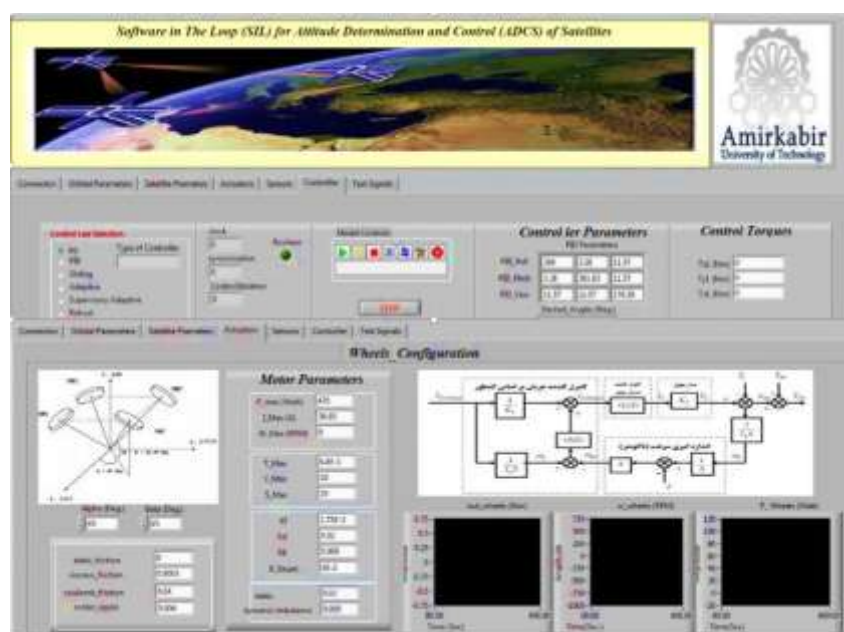


Figure 1. Graphical user interface

In the designed test bed, RS232 serial communication protocol has been used to transfer data between simulator computer and on-board electronic. Designed processor in the loop test bed operate as follow: at first, technical specification of the satellite, including the moment of inertia, mass and geometric properties, initial conditions of attitude and angular velocity of satellite after launch, desired attitude and maneuvers, orbital characteristics and specifications of reaction wheels and gyros, should be defined in graphical user interface processor. In this structure, the attitude determination information will provided by DLL file corresponding to dynamics model of the satellite. Then attitude information transferred to the on-board electronics through the serial port. On-board electronics uses these data to compute control torque and reaction wheels torques using attitude control algorithm based on receiving data including attitude and angular velocity of satellite. Calculated control torques transferred through the serial port to simulator computer and in DLL model, new attitude of the satellite will be computed. This loop will continue in real-time condition. Figure 2 shows a closed loop diagram of the implemented processor in the loop test bed and Figure 3 shows hardware in the loop test bed and equipment including simulator computer, RS232 cable and on-board electronic.

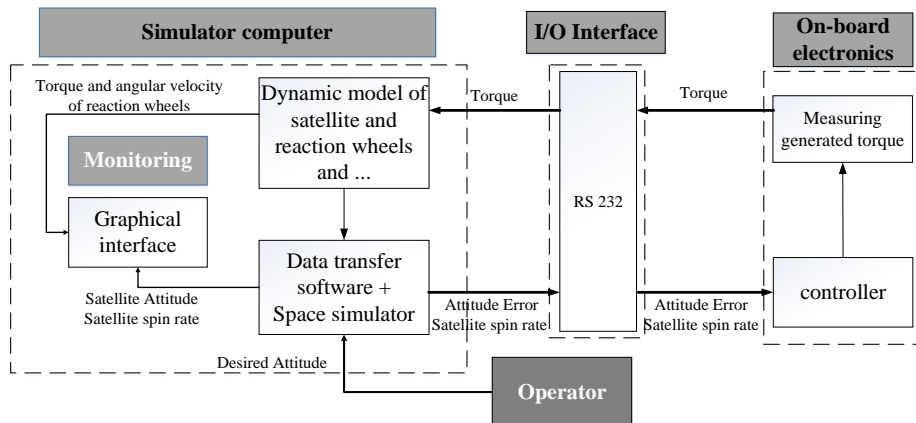


Figure 2. Closed loop functional block diagram of processor in the loop test bed

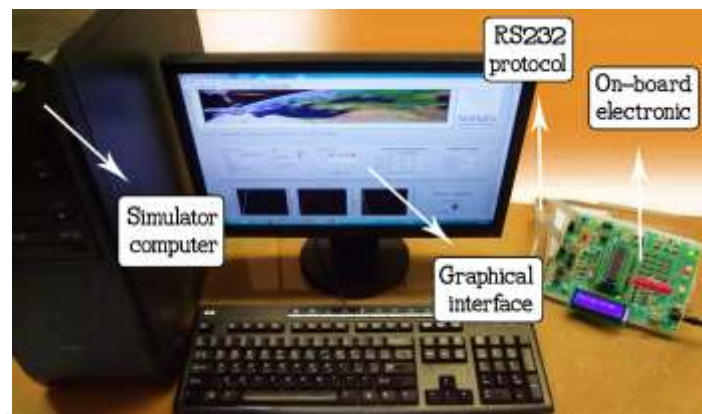


Figure 3. processor in the loop test bed equipment

VI. IMPLEMENTING ATTITUDE CONTROL ALGORITHM IN THE PROCESSOR IN THE LOOP TEST BED

In this section, the results of the processor in the loop (PIL) tests for designed backstepping sliding mode control algorithm are presented and then compared with the simulation result of designed controller in MATLAB/Simulink environment to demonstrate the capabilities of the mentioned algorithm in a real-time situation. In these tests, the spacecraft attitude determination data is extracted directly from simulation model and sampling time of the control loop is 0.4 seconds. These simulations are carried out for a LEO satellite with the altitude of 750 km and orbit inclination of 98.2° . Inertia momentum matrix respect to body reference frame is assumed $I = \text{diag} \{1000, 500, 700\}$ and controller parameters and characteristics of reaction wheels according with specification states in reference (Bolandi, et al., 2010) are listed in Table 1. Desired Euler angles are assumed $\psi_d = 0^\circ, \theta_d = 25^\circ, \phi_d = 20^\circ$. Figure 4 to Figure 6 show the results of our proposed backstepping-sliding mode controller which is implemented in processor in the loop test bed in presence of actuator dynamics and environmental disturbances compared with the simulation results. Figure 7 and Figure 8 show output torque of reaction wheels and angular velocity of reaction wheels, respectively. Also 25 percent uncertainties on the moments of inertia have been considered to demonstrate the robustness of the controller.

Table 1. Simulation parameters

Reaction wheel		Backstepping-Sliding mode controller	
Maximum torque (T_{\max})	0.75 (N.m)	λ	-0.5
Maximum power (P_{\max})	470 (W)	k	0.005
Maximum current (I_{\max})	38.85 (A)	ε	0.05
Maximum angular velocity (ω_{\max})	6000 (RPM)		

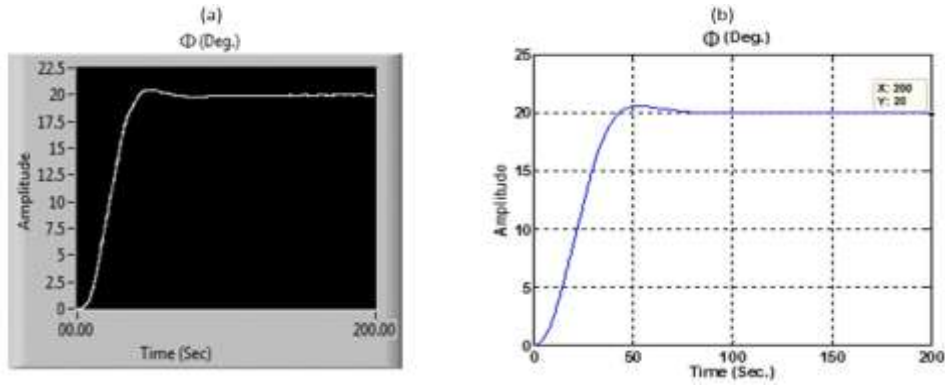


Figure 4. Performance of backstepping-sliding mode controller for roll axis a) Implementation b) simulation

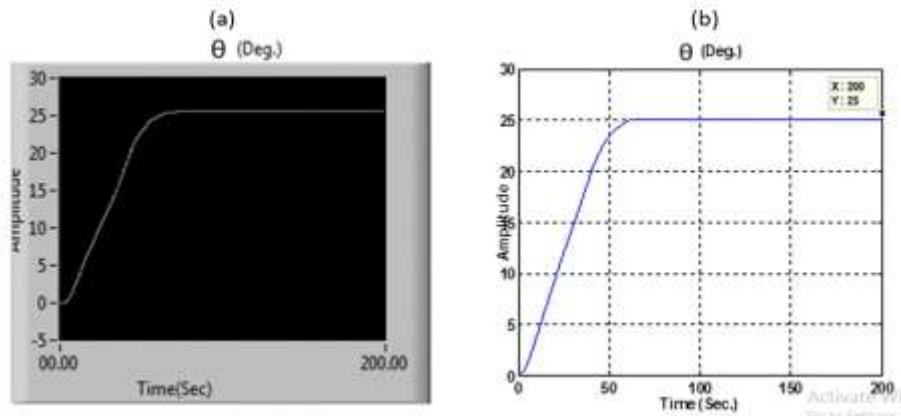


Figure 5. Performance of backstepping-sliding mode controller for pitch axis a) Implementation b) simulation

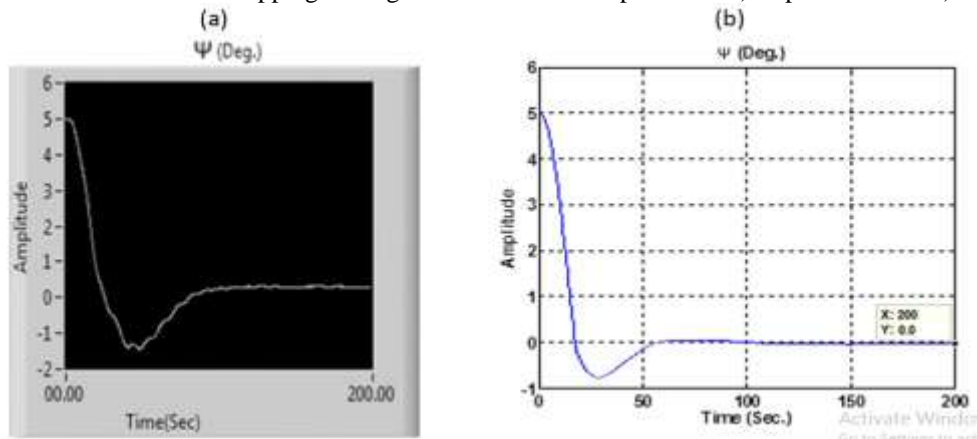


Figure 6. Performance of backstepping-sliding mode controller for yaw axis a) Implementation b) simulation

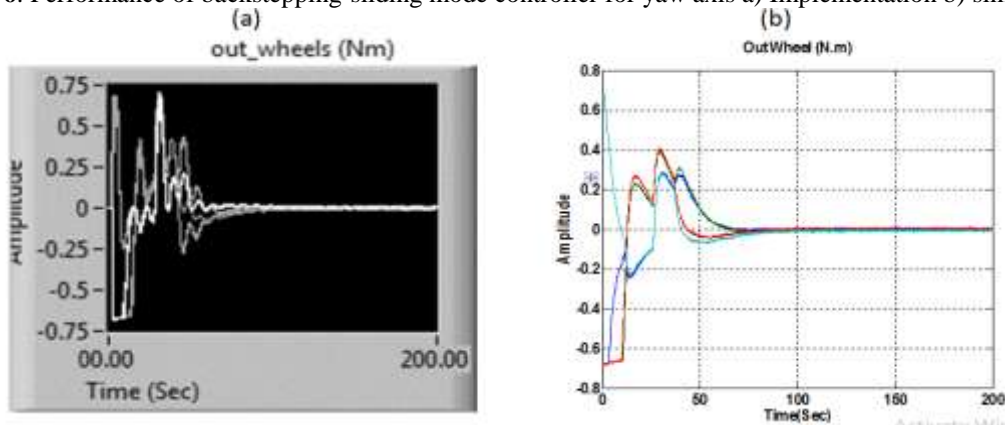


Figure 7. Output torques of reaction wheels a) Implementation b) simulation

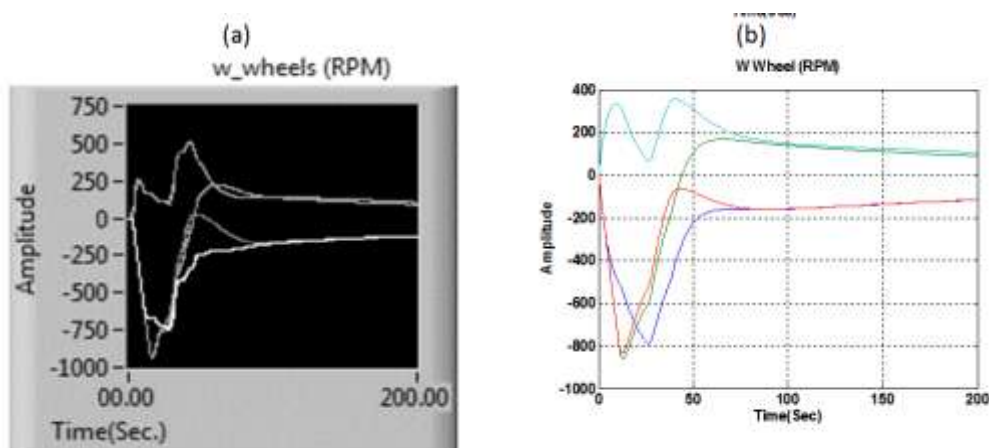


Figure 8. Angular velocity of reaction wheels a) Implementation b) simulation

As it can be seen designed backstepping-sliding mode controller despite 25 percent of uncertainty on moment of inertia, unknown disturbances, actuator dynamics works properly and designed processor in the loop test bed are capable of executing control law accurately. Comparing simulation and implementation result show some deviation among these results. The major source of deviation is originated from delay time corresponding to transmission data between on-board electronic and simulator computer. Note that since in real operation in orbit, there is no need to transfer data between the on-board electronic and the computer, so the mentioned error is not problematic.

VII. CONCLUSION

In this paper, a robust attitude control algorithm was developed based on backstepping-sliding mode control for a satellite using four reaction wheels in a tetrahedron configuration. Backstepping sliding mode controller is composed of a robust term for attitude stabilization in presence of unknown inertia and external disturbance, and a backstepping term for eliminating the effects of actuator dynamics model. In this method, asymptotic stability of the proposed algorithm was proven in the presence of reaction wheels dynamics model based on Lyapunov theory. Then, in order to verification and evaluating the performance of the proposed algorithm, a low-cost real-time processor in the loop test bed was provided. Then the proposed control algorithm performance was investigated by implementing it in an electronic control board of the processor in the loop test bed and proper performance of the designed algorithm in performing control mission was illustrated by PIL real-time test. However there are some deviations between simulation and practical results but these deviations are not critical and the proposed algorithm achieve attitude control mission properly.

REFERENCES

- [1] T. v. Chelaru, B. Cristian and A. Chelaru, Mathematical model for small satellites, using rotation angles and optimal control synthesis, in Recent Advances in Space Technologies (RAST), Istanbul, Turkiye, 2011.
- [2] H. Qinglei, Sliding mode maneuvering control and active vibration damping three axis stabilized flexible spacecraft with actuator dynamics, *Nonlinear Dynamics*, 15, 2008, 227-248.
- [3] Y. Jin, X. Liu, W. Qiu and C. Z. Hou, Time-varying Sliding Mode Control for a Class of Uncertain MIMO Nonlinear System Subject to Control Input Constraint, *Science China, Information Science*, 53(1), 2009, 89-100.
- [4] H. Qinglei, Robust Adaptive Sliding Mode Attitude Maneuvering and Vibration Damping of Three Axis Stabilized Flexible Spacecraft With Actuator Saturation Limits, *Nonlinear Dynamics*, 55, 2009, 301-321.
- [5] M. Moradi, Self-tuning PID controller to three-axis stabilization of a satellite with unknown parameters, *International Journal of Non-Linear Mechanics*, 49, 2013, 50-56.
- [6] M. Shahravi, M. Kabganian and A. Alasty, Adaptive robust attitude control of a flexible spacecraft, *International Journal of Robust and Nonlinear Control*, 16(6), 2006, 287-302.
- [7] P. Guan, X.-J. Liu and J. Z. Liu, Adaptive fuzzy sliding mode control for flexible satellite, *Engineering Applications of Artificial Intelligence*, 18(4), 2005, 451-459.
- [8] Z. Song, H. Li and K. Sun, Finite-time control for nonlinear spacecraft attitude based on terminal sliding mode technique, *ISA Transactions*, 53(1), 2014, 117-124.
- [9] G. Hu, Variable Structure Maneuvering Control with Time-Varying Sliding Surface and Active Vibration Damping of Flexible Spacecraft with Input Saturation, *Acta Astronautica*, vol. 64, pp. 1085-1108, 2009.
- [10] J. D. Bošković, S. M. Li and R. M. Mehra, Robust Adaptive Variable Structure Control of Spacecraft Under Control Input Saturation, *JOURNAL OF GUIDANCE, CONTROL, AND DYNAMICS*, 24(1), 2001, 14-22.
- [11] H. Qinglei, L. Bo and Z. Aihua, Robust Finite-Time Control Allocation in Spacecraft Attitude Stabilization under Actuator Misalignment, *Nonlinear Dynamics*, 53(1), 2013, 53-71.
- [12] S. R. Vadali, Variable Structure Control of Spacecraft Large Angle Maneuvers, *Journal of Guidance, Control and Dynamics*, 9, 1986, 235-239.

- [13] T. A. W. Dwyer, H. S. Ramirez, S. Monaco and S. Stornelli, Variable structure control of globally feedback-decoupled deformable vehicle maneuvers, in 26th IEEE Conference on Decision and Control, Los Angeles, California, 1987.
- [14] R. D. Robinett and G. G. Parker, Spacecraft Euler Parameter Tracking of Large-Angle Maneuvers via Sliding Mode Control, *Journal of Guidance, Control, and Dynamics*, 19(3), 1996, 702-703.
- [15] S.-N. Wu, X.-Y. Sun, Z.-W. Sun and C.-C. Chen, Robust sliding mode control for spacecraft global fast-tracking manoeuvre, *Journal of Aerospace Engineering*, 225, 2011, 749-760.
- [16] K. Lu, Y. Xia, Z. Zhu and M. V. Basin, Sliding Mode Attitude Tracking of Rigid Spacecraft with Disturbances, *Journal of the Franklin Institute*, 349, 2012, 413-440.
- [17] H. S. Ramirez and T. A. W. Dwyer, Variable Structure Control of Spacecraft Reorientation Maneuvers, in *Proceedings of AIAA Guidance, Navigation, and Control Conference*, Williamsburge, 1986.
- [18] S. R. Marandi and V. J. Modi, A Preferred Coordinate System and Associated Orientation Representation in Attitude Dynamics, *Acta Astronautica*, 15, 1987, 833-843.
- [19] M. D. Shuster, A Survey of Attitude Representations, *The Journal of the Astronautical Sciences*, 41, 1993, 439-517.
- [20] H. Bolandi, M. Haghparast, F. F. Saberi, B. G. Vaghei and S. M. Smailzadh, On-Board Electronic Of Satellite Attitude Determination and Control Subsystem: Design and Test in Hardware in the Loop Test Bed, *The Journal of Institute of Measurement and Control*, 45(5), 2012, 151-157.
- [21] M. J. Sidi, *Spacecraft Dynamics and control: a practical engineering approach* (Cambridge: Cambridge University Press, 1997).
- [22] J. Crassidis and F. Markley, Sliding Mode Control Using Modified Rodrigues Parameters, *AIAA Journal of Guidance, Control and Dynamics*, 19(6), 1996, 1381-1383.
- [23] K. Lu, Y. Xia, Z. Zhu and M. V. Basin, Sliding Mode Attitude Tracking of Rigid Spacecraft with Disturbances, *Journal of the Franklin Institute*, 349, 2012, 413-440.
- [24] Q. Hu, Sliding mode attitude control with L2-gain performance and vibration reduction of flexible spacecraft with actuator dynamics, *Acta Astronautica*, 67(5), 2012, 572-583.
- [25] H. Bolandi, F. F. Saberi and A. E. Mehrjardi, Design of Attitude Control System of a Satellite with Large Angle Maneuvers Considering of Reaction Wheels Model and Restrictions, *Journal of Space Engineering*, 1(1), 2011.
- [26] J. Wertz, *Spacecraft Attitude Determination and Control* (London: Kluwer Academic, 1978).
- [27] H. Bolandi, F. F. Saberi and B. G. Vaghei, Design of a Supervisory Adaptive Attitude Control (SAAC) System for a Stereo-Imagery Satellite Based On Multiple Model Control with Switching, *International Journal of Innovative Computing, Information and Control*, 6(9), 2010, 4675-4692.